Scientia Iranica D (2022) 29(6), 3304–3316

Sharif University of Technology
Scientia Iranica
Transactions D: Computer Science & Engineering and Electrical Engineering
http://scientiairanica.sharif.edu

An inset-feed on-chip frequency reconfigurable patch antenna design with high tuning efficiency and compatible radome structure for broadband wireless applications

R. Kumar Verma[a], R.L. Yadava[b], and D. Balodi[c,*]

a. *Electronics and Communication Engineering Department, Amity University, Uttar Pradesh, India.*
b. *Electronics and Communication Engineering Department, Galgotias College of Engineering and Technology, G. Noida, India.*
c. *Electronics and Communication Engineering Department, BBD Engineering College, Lucknow, India.*

Received 18 June 2020; received in revised form 1 December 2020; accepted 15 March 2021

KEYWORDS
Microstrip;
PIN diodes;
Patch;
Radiation pattern;
Reconfigurability;
Bandwidth.

Abstract. A novel, dual-edge-shape frequency reconfigurable antenna with a highly compact size is proposed using microstrip line-based inset-feed mechanism. The proposed antenna uses the cost-effective Roger substrate of 0.787 mm thickness. Tuning reconfigurability was achieved using two PIN diode switches placed on the patch surface. The ON-OFF switching combinations of the PIN diodes provided variations in the current distribution and thereby, altered the resonant frequencies. The proposed antenna offers a resonating spectrum in the range of 3 GHz to 9 GHz, approximately, with the maximum tuning efficiency of 43% at 6.5 GHz, covering a majority of modern RF standards. The patch antenna design radiates with a reasonably high gain of 2.3 dBi at 5.04 GHz, with the effective bandwidth of 2800 MHz (maximum at 6.5 GHz). The proposed multiband antenna with radome structure (ABS material) was investigated in the high-frequency simulation environment of ADS-Keysight Technologies and the 3D radiation pattern (far-field gain, directivity, and power calculations) was obtained using momentum and Electro-Magnetic Design Simulator (EMDS). The final implementation size (without radome structure) was 23 mm $\times$ 26 mm (595 mm^2). The proposed design with uniform far-field radiation pattern would pave the way for better wireless applications, including WLAN and WiMAX communications.

1. Introduction

With rapid increase in the application of modern RF integrated circuits to the recent wireless systems, compatible and reconfigurable wideband antenna solutions are being sought very frequently. A key design challenge is to choose the right antenna for a specific application. Power efficiency and impedance bandwidth are the most important parameters, which an RF engineer would like to work upon, in this regard. The exponential increase in the demand for the internet of things and the brilliant modern applications impose numerous scientific and engineering challenges that require smart research efforts from both academia and industry to improve efficiency, cost-effectiveness, scalability, and reliability of the IoT antenna systems.

Antenna systems are used in improving the field

*. *Corresponding author.*
E-mail addresses: vermarahul75@gmail.com (R. Kumar Verma); rlyadava.vps@gmail.com (R.L. Yadava); deepakbalodi@gmail.com (D. Balodi)

doi: 10.24200/sci.2021.56226.4612

of IoT and in numerous applications including remote sensing, satellite communication, navigation systems, GPS, etc. In most of the modern wireless systems, the conventional practice of using multi-antenna patches for wider and multi-band coverage has been avoided. Instead, the radiation spectrum has been reconfigured by multi-band reconfigurable antenna design, which is able to resonate at multiple desired frequencies. In addition to the compactness in die-size, this design type also helps reduce the overall cost of the RF-front end system on a chip or SoC. A major focus of the design effort in this area has also been devoted to enhancing bandwidth (broader spectrum) and multi-band reconfigurability of the patch antenna. The conceptual idea of a patch antenna based on the microstrip-line concept is shown in Figure 1. Wider spectrum coverage has become an essential feature of modern communication systems due to the high data rates and other emerging trends in wireless standards. These modern wireless standards demand for the reconfigurability of the antenna for its diverse applications and coverage range. This is in addition to the demand for reduction in bandwidth coverage in cellular applications, extensive inception of spread-spectrum signals, and employing bandwidth-efficient modulation techniques.

The recent trends and techniques of wireless tuning of cellular bands have therefore been toward avoiding the simultaneous application coverage. Furthermore, when frequency reconfigurability is necessary, the functionality of patch antenna is improved by keeping the size small and the design less complicated (important geometries are shown in Figure 1). Frequency reconfigurable patch antennae hold certain other necessary constraints as characteristics to them than compact size, which include compatibility with the analog-RF front end systems and quick hopping between resonating bands. These features help them efficiently serve in most of the modern wireless communication systems.

Different modern techniques for antenna reconfiguration have been illustrated by Shakhirul et al. [1]. A comprehensive and detailed review of microstrip reconfigurable antennae was provided along with a subjective discussion of the pros and cons of their wideband applications. The work offered by Shakhirul also entailed the switching behavior of the RF switches and made an effort to enhance their switching at different frequency bands. Frequency reconfigurability by the change of operative length of the patch antenna has been dealt with by most of the researchers. Several researchers have attained frequency reconfiguration by changing the operative length of the antenna by removing from or adding to its length through various approaches, such as varactors or variable capacitors. A work by Rahman et al. [2] reported the incorporation of a varactor in the patch design and enhanced the bandwidth to a greater extent. The surface currents were redirected by varactor diodes, which ultimately brought in the frequency modulation with capacitive variation. A similar approach was reported in the work by Li et al. [3]. In some other similar works, a high degree of impedance matching has been achieved in the spectrum of 890 MHz to 1500 MHz. Several other articles have designed antennae that compromise abilities to incorporate the 50 Ω impedance [4,5].

Antennae have shown promising performances when multiple smaller patches are connected using varactors, offering ease of switching between multiple polarizations of the work, frequency tuning, and phase shifting. Korosec et al. [5] presented a different multi-sub-patch microstrip antenna loaded with varactors for solving a reconfiguration problem. In addition to

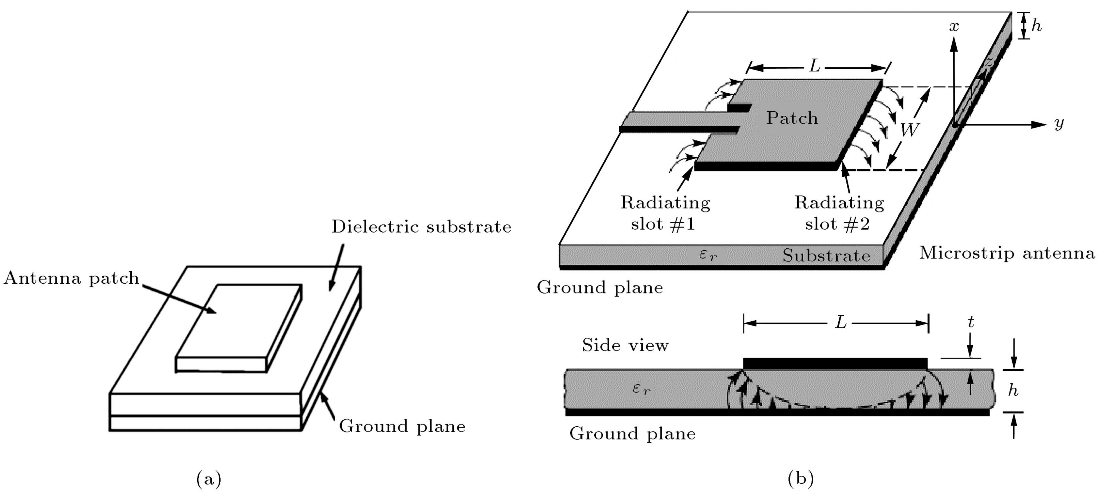

Figure 1. Microstrip patch antenna: (a) The conventional structure consisting of a radiating patch on one side of the dielectric substrate and ground plane on the other side and (b) ample rectangular patch with dimensions and associated fields.

the frequent usage of PIN and varactor devices, RF Micro-Electro-Mechanical Systems (MEMSs) offer high Q tuning performance along with low losses in the wideband applications [6]. Amongst these switching techniques, PIN diodes are very consistent and compact as they tend to increase switching speeds and decrease resistive capacitance in both ON and OFF states. The slot lengths are also switched particularly in the CPW fed antenna and folded slot antenna to change the resonant frequency as a reconfigurable phenomenon. One such approach has been presented by Nguyen-Trong et al. [7].

In the conventional integration of heterogeneous front-end wireless systems, multichip module and System-in-Package (SiP) solutions can suffer from large antenna size [8]. Furthermore, an in-package antenna flip-chipped on a transceiver module substantially increases its packaging cost [9,10]. Also, package integration becomes more challenging with the increasingly lossy interconnects such as wire-bonds and solder bumps [8]. As an alternative to the SiP, a System-on-Chip (SoC) approach integrates the complete RF front-end with an on-chip antenna directly on the same silicon die in a so-called Antenna-on-Chip (AoC) design, thereby avoiding lossy interconnections. Besides, compared to SiP, AoC reduces the reliability dependence on manufacturing precision [11]. The SoC advancements and applications to modern Very-Large-Scale Integration (VLSI) solutions have invited more and more antenna utilization in higher spectra. Q-band on-chip antennae with high gain and wide band are a result of such efforts.

The use of a substrate of high resistivity and low dielectric constant reduces the losses by minimizing the radiation and current leakage to the other on-chip components in patch antenna implementation. In a work [12], the major effort was to improve the antenna gain (achieving around -1.8 dBi) by employing a high-resistivity silicon substrate in association with CMOS-SOI (Silicon On Insulator) technology. Another effort [13] was made to employ an off-chip dielectric resonator with high permittivity by placing it on the top of the chip. An H-slot was designed and implemented to excite the dielectric resonator, which finally resulted in the antenna gain of 1 dBi (closed to what was expected in the simulation). Furthermore, a triangular patch antenna was designed and implemented [14] to meet the Q-LINKPAN standards. Its implementation in the standard CMOS process with the approximate gain of 1.5 dBi (at central frequency of 45 GHz in simulations) made it quite reasonable and market-efficient for the spectrum range of 40-50 GHz applications. In a very recent attempt [15], a monolithic on-chip antenna was designed and optimized with Back-End-of-the-Line (BEoL) challenges of the nanoscale technology for 5G applications using mm-wave. The high radiation efficiency of 37.3% and power gain of 9.8 dB were achieved by the use of ground metallization on a PCB board, which served as a reflector.

The compatibility of a microstrip-based design line by the conventional CMOS technology implementation has been a major bottleneck since long. This is perhaps the major reason why the development of RF integrated circuits and especially the patch antenna design have followed their own design routines by microstrip and high-k-substrate-based off-chip implementation [16]. Wherever possible, the CMOS integrity demands a greater effort towards preventing noise and signal attenuation, as explained in [16,17], by the conventional design style of CMOS-based Low Noise Amplifier (LNA) circuit. The LNA design aims for the same spectrum range as that of the proposed patch antenna design in the present study. A compact front end solution, demanded by the 5G communication, further complicates this constraint in on-chip CMOS implementation of patch antenna. A recently published article [17] emphasized this issue and offered a solution in nanoscale 28 nm- CMOS technology for millimeter-wave (mm-wave) applications. Due to its high mobility ratio and fast turn ON characteristic, PIN diode is the most favorable RF switch for the frequency reconfigurable antennae sought today in modern wireless systems. The PIN diode based switchable microstrip patch antenna has been presented in some recently published works [18,19] for WLAN/Wimax applications. The miniaturized dual-band microstrip patch antenna array in [18] resonates at 2.2 GHz and 3.8 GHz, whereas a frequency-reconfigurability was obtained in [19] using six PIN diodes positioned symmetrically along the non-radiating edges. Both the works offer a highly compact solution with stable and directional patterns obtained on a single-layer substrate. Another frequency reconfigurable work based on 0.18-μm CMOS-SOI process [20] also presented an on-chip antenna solution for the broadband characteristic. A bandwidth of -10 dB was obtained for Q-band operation (29.5 GHz to 51.0 GHz) by toggling the state of the on-chip switches.

A typical inset feed mechanism for better impedance matching is presented in the present article. Two similar rectangular patches are designed and selectively shortened using the PIN diode-based switches to enhance the bandwidth of the proposed patch antenna design. The effective length of the radiating patch is moderated by changing the states of the two on-chip RF diode-based switches. The resonating spectrum of the whole patch antenna (along with the switches) shifts according to the effective length (i.e., according to the states of the diodes) and thereby, the whole bandwidth of the proposed antenna changes. The selection of a reasonable gate width is also a considerable task as the resonating bandwidth and antenna gain depend upon the gate width of the switches. Design simulations were carried out to achieve the optimum value of the gate width. Section 2 describes the basic development and theoretical support behind the design, starting from the inset feed topology to on-chip PIN diode incorporation. Then, quantitative developments and calculations for the integrated patch will be presented. Section 3 briefly presents the reasoning behind the selected radome structure and argues the impact of its application. Finally, Section 4 presents the actual design implementation along with high-frequency simulation setup and measurement results. It is shown that the proposed antenna has a favorable −10 dB impedance bandwidth from 3 to 9 GHz, approximately, in multiple-band segments. The tuning of bands was done by reconfigurability of the proposed design. A promising measured gain of −2.3 dBi at 5.12 GHz was obtained in one of the tuned bandwidths. In addition to the above-mentioned features, a highly compact die size 595 mm^2 was achieved.

2. Integrated on-chip antenna design

The section demonstrates the complete patch antenna design by the proposed inset feed line. Both the structures are compatible with microstrip topology and implemented with a metal line of chosen specifications.

2.1. Inset feed design calculations

The feeding of antenna is as important as its patch design given that feed design and insertion provision affect the overall performance characteristics of antenna design, including the radiation pattern. Two conventionally used feeding mechanisms for the microstrip patch antenna are coaxial probing and inset microstrip line. Coaxial probe feeding is sometimes advantageous for applications like active antennae, while microstrip line feeding is suitable for developing high-gain microstrip array antennae [15]. In both cases, the probe position or the inset length determines the input impedance. By using a straightforward transmission-line model, it is possible to accurately model and analyze microstrip-line inset-fed patch antenna designs [15,21]. For a 50-Ω input impedance, the calculations could be carried out to get exact inset length and location of feed joint at the patch through the curve-fitting approach.

For a patch to work on a targeted range of spectra (mm-wave applications of S and C bands), the design geometry of feed line is calculated for a Roger substrate (Roger 5880) of height H (or h) = 0.787 mm and loss tangent ($\tan D$) of 0.0009. The copper is the selected metal with a thickness of T = 35 μm. The inset feed length is given in Eq. (1) for the conventional range of dielectric strength ($2 \leq \varepsilon_r \leq 10$):

$$y_o = 10^{(-4)}\Big\{0.001699\varepsilon_r^7 + 0.1376\varepsilon_r^6 - 6.1783\varepsilon_r^5 + 93.187\varepsilon_r^4 - 682.69\varepsilon_r^3 + 2561.9\varepsilon_r^2 - 4043\varepsilon_r + 6697\Big\}. \quad (1)$$

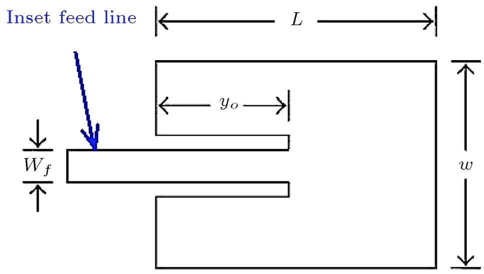

Figure 2. Inset feed line with a prototype patch antenna.

The fringing effects, substrate imperfections, and feeding leakages affect the ε_r presented in Eq. (1). Hence, the following equation presents a more practical value of the effective dielectric strength (ε_{eff}) for the width of the proposed patch (W) when it is higher than the height of the substrate (H or h):

$$\varepsilon_{eff} = \frac{(\varepsilon_r + 1)}{2} + \frac{(\varepsilon_r - 1)}{2}\left[1 + 12\frac{h}{W}\right]^{(-1/2)}. \quad (2)$$

A manual iterative calculation can lead to a feasible geometry solution for the inset feed length and width. For this purpose, the line-calc (ADS) was employed, which inherently made use of the above equations. The roughly approximated patch line and width of 24 mm and 20 mm were considered to utilize the above equations in the calculator. This gave the effective dielectric strength (ε_{eff}) value of 2.095. The lower value of ε_{eff} than ε_r was due to the leakage through fringing and feeding imperfections and substrate anomalies. The exact calculations of W and L will be presented in the upcoming subsections.

Using the above initial estimations for patch line and width along with the modified dielectric strength in the line-calculator, the inset feed line length (y_o) and width (W_f) came out 10.934 mm and 2.375 mm, respectively (Figure 2, the prototyped model). The obtained dimensions were in complete agreement with the compact nature of the complete design target. The actual feed point connections to the patch would be handled after finalization of the patch dimensions. A conventional topology of central contact was adopted to minimize the leakage and maximize the gain of the antenna. This again elucidates the utility of the microstrip line based inset feed.

2.2. PIN diode model and inception

The PIN diode has been the primary choice of RF circuit designers for several decades as a unique high-frequency tool capable of handling high EM power. This is while it uses only a very small amount of current

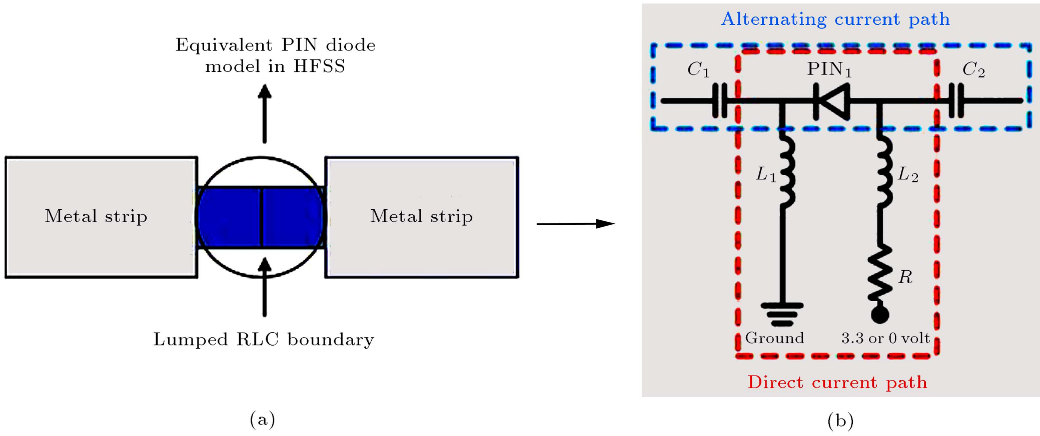

Figure 3. PIN diode: (a) Layout-equivalent model in HFSS and HPEESOF (ADS for momentum) and (b) equivalent circuit model (on-chip model) with coupling circuitry.

to control the huge radiated power, which makes it suitable for low-power RF and microwave circuit implementation. The segment sandwiched between the two sides of the doped semiconductor in PIN diode construction is called the intrinsic region, which shows a smaller and linear junction capacitance, even at very high frequencies (modern RF spectrum). This makes the PIN diode suitable for the implementation of RF/microwave attenuators. An important limitation, however, in the modeling of PIN diode behavior is to find a consistent model ubiquitously. This constraint in the complicated switching behavior of the PIN diode makes it quite difficult for most of the circuit simulators to precisely model the transition characteristics. The variety of the RF applications and circuit behavior leads to the variation in the construction and exact implementation of PIN diodes. Given that in most of the RF applications, the switching behavior of the *PIN* diode is incorporated, the thin intrinsic region of the diode is the major focus in its construction. By controlling the forward current, a range of attenuation values can be achieved [22,23]. The excellent characteristics of the PIN diodes including wider bandwidth, high-power handling capability, and compactness in design make them the first choice in RF switches. Figures 3 and 4 show the PIN diode construction and its forward and reverse bias equivalent circuits [23,24].

Figure 3(a) demonstrates the terminal equivalence of the PIN diode switch modelled in the layout geometry. Herein, the distributed impact of PIN geometry has been equated with the lumped passive characterization (Figure 3(b)). The opted PIN diode at low frequencies (below the transit time-frequency of the I-region) behaves like a conventional silicon *PN* junction diode. Out of certain important parameters, the forward voltage drop of a PIN diode is generally the most important consideration. The switching behavior of the PIN diode current is utilized to remove the stored charge Q, which gets accumulated in the forward

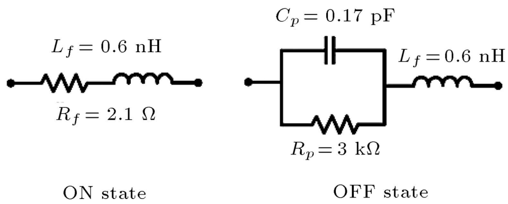

Figure 4. Equivalent operational model of PIN diode (BAR64-02) under ON and OFF stages.

biased condition. For this to happen, the incremental stored charge must definitely be lower than the junction stored charge Q and hence, be easily wiped out by the RF current [25]. Another important parameter is the maximum reverse bias rating V_R as a permissible limit. Apart from the regular forward and reverse bias ratings, the breakdown mechanism also offers the noticeable parameter of breakdown voltage V_B corresponding to the avalanche effect. Therefore, in a typical application, maximum negative voltage swing should never exceed V_B. An instantaneous excursion of the RF signal in the positive bias direction generally does not cause the diode to go into conduction because of the slow reverse-to-forward switching speed, T_{RF}, of the *PIN* diode.

Figure 4 simplifies the operational model of a PIN switch and provides a totally clear presentation of the functionality of the lumped model. The opted BAR6402 PIN diode behaves as a conventional RL series combination in ON mode and RC parallel along with series L in OFF mode (the obtained values for the passive components are given in Figure 4), wherein the high value of the resistor in OFF mode offers the cutoff topology from the remaining patch edge as shown in Figure 5.

2.3. Patch geometry and design integration

This section discusses the patch design geometry calculations, which so far constitute the most crucial step and core part of the microstrip patch antenna design.

Table 1. Dimensions of the proposed patch antenna (all values are in mm).

Parameter	L	L_1	L_2	L_3	L_4	L_f	y_0
Dimension (mm)	20	3	6	3	5	5	4
Parameter	W	W_1	W_2	W_3	W_4	W_f	$C1$, $C2$
Dimension (mm)	22	7	6	4	2	2	PIN switch connections

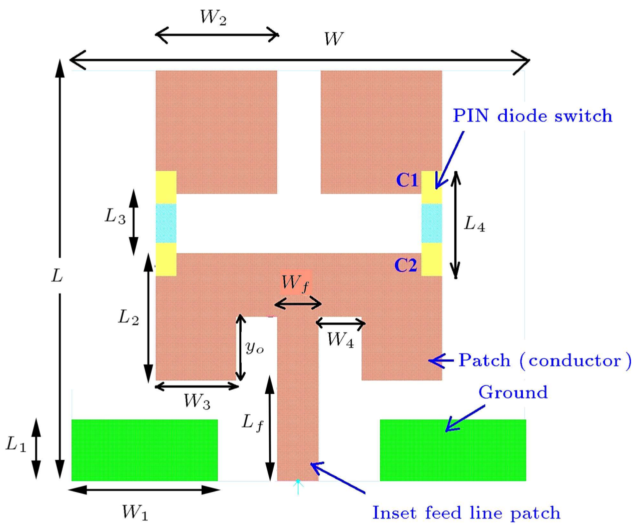

Figure 5. Design geometry of the proposed reconfigurable patch (D with C_1 and C_2 terminals represents the PIN diode implementation).

The width and length of the patch are conventionally given by the following equations:

$$W = \frac{1}{2f_T\sqrt{\mu_o\varepsilon_o}}\sqrt{\frac{2}{\varepsilon_r+1}}, \tag{3}$$

$$L = \frac{1}{2f_T\sqrt{\mu_o\varepsilon_o\varepsilon_{eff}}} - 2\Delta L. \tag{4}$$

The first initial guess for the width is made using Eq. (3) with ε_{eff} of the value 2.095 from Eq. (2). This gives an approximate antenna width (W) of 23 mm for the most sought application of 5.4 GHz (for wireless LAN, WiFi) in the targeted band of operation. The patch length (Eq. (4)) deals with fringing leakage and substrate irregularities, whereas only insignificant effects on patch width are observed. The effect of leakage and other parasitic anomalies are incorporated in channel length via a length corrective parameter ΔL, given in Eq. (5):

$$\frac{\Delta L}{h} = 0.412\frac{(\varepsilon_{eff}+0.3)\,.\,(\frac{W}{h}+0.264)}{(\varepsilon_{eff}-0.258)\,.\,(\frac{W}{h}+0.8)}. \tag{5}$$

ΔL in Eq. (5) is taken from Eq. (4) as a corrective parameter, which finally provides a patch length of $L = 26$ mm. It can be observed from the above practice that obtaining patch width (W) is subject to iterative calculations, whereas patch length (L) is obtained straightforwardly. Patch width thereby accounts for the antenna gain and directivity in a more significant manner. The idealistic scenario for any patch geometry of the microstrip antenna is to maintain $W \gg h$, where W is the approximate patch width and 'h' is the substrate height (or thickness). Even though it is impractical to have this idealistic scenario in most of the practical designs, the planar IC practices tend to comply with this condition in close proximity. The final designed patch along with inset feed and on-chip PIN switches is shown in Figure 5, wherein the geometrical dimensions of the proposed antenna designs could easily be identified. The patch dimensions are also listed in Table 1.

Roger-5880 (RT/Duroid) materials have been of extensive use as a substrate in RF applications for two decades. The excellent characteristics including low loss and low cost of the Roger–5880 substrate were also observed in the present study besides other characteristics, which were tangent of tan $D = 0.0009$, dielectric constant of $\varepsilon_r = 2.2$, and thickness of 0.787 mm. The overall dimensions of the antenna were 23 mm × 26 mm. The antenna design modelling was carried out in a commercially available FEM (Finite Element Method)-based simulator, *ADS-HPEEsof*, and *momentum*. A dual-edge rectangular shape was used for the designed patch to achieve high gain and better impedance matching. Also, the inset feed line was connected to the central feed point of the lower edge of the patch, as shown in Figure 5. The spectrum reconfigurability and wide-band coverage were maintained with the help of the *PIN* diodes (shown with yellow strips in Figure 5), with a lumped element boundary in a reserved slot of 1 mm.

3. Integrated design with radome structure

Metamaterials have attracted great interest in the field of antenna design mainly from the year 2000 onwards [26–28]. They are a class of materials that exhibit unique properties which materials existing in the nature do not possess. A metamaterial cover can efficiently improve antenna directivities with accurate selection of the working frequency and the cover dimensions. The metamaterial cover termed as radome has a congregating effect on the transmission direction of the EM wave, which is similar to the congregation effect of a convex lens on the radiation of light wave. Under ideal conditions, the larger cover size of the metamaterial and the higher number of layers is more desirable. However, under actual conditions, one must use the lowest space resource to obtain the best function of the antenna [29,30] and for this special purpose, Newton's divided difference method is used.

Radome is an associated Frequency Selective Structure (FSS) to further improve antenna radiation and efficiency by providing band-pass selectivity in the electromagnetic domain. An ideal radome structure is expected to remain electromagnetically transparent to the desired frequency bands of operation and offer significant attenuation of the out-of-band radiations. In addition to improving radiation efficiency, a radome structure is also expected to strengthen the physical strata of the antenna geometry. By the virtue of this, it helps protect radars against the odds of physical environment. This finally reduces the operational cost of the implemented antenna and provides durability as well [31]. Frequency-selective radome structures are generally employed in curved shape with compact size to keep compatibility with the physical neighborhood of the antenna. However, the close proximity requiring to maintain the compactness of the antenna also brings in the mutual coupling effect between the antenna and the radome structure, which cannot be neglected in practical applications. This coupling phenomenon also impacts the radiation performance of the antenna already planned [32]. The wet and humid conditions (for instance, in the presence of water and/or ice) may further degrade the strength of radio signals that are in the desired band, due to the susceptibility of the radome structure. Radome FSS significantly deteriorates the radar signals, but the exact performance and amount of attenuation depend upon the operating frequency and physical elements of the radome implementation [33]. Therefore, it is recommended to meet the specific constraints related to these degradations in the radome *FSS* based antenna implementations, especially in the mm-wave systems. This further demands higher directivity from the implemented patch antennae to compensate for the aforementioned degradations.

In this paper, an FSS radome is proposed to improve the patch antenna gain and make it more directive without any significant loss of gain, as shown in Figure 6. The proposed *FSS* radome was used as an additional layer. The radome structure was purposely placed in the proximity of the near-field region of the patch antenna. In this work, the patch antenna and *radome structure* were designed as separate units to keep the dimensional and radiation pattern control intact. A very popular and conventional ABS plastic material was used for the analysis of the radome structure and in the simulation.

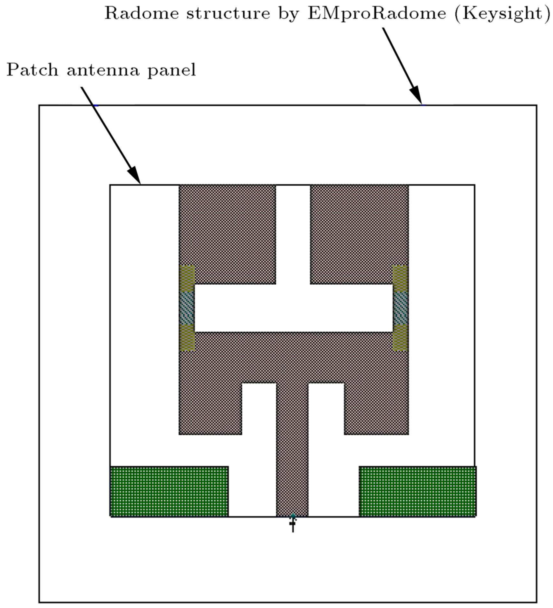

Figure 6. Patch antenna with the proposed radome structure (modelled by EMProRadome_DesignKit of keysight technology).

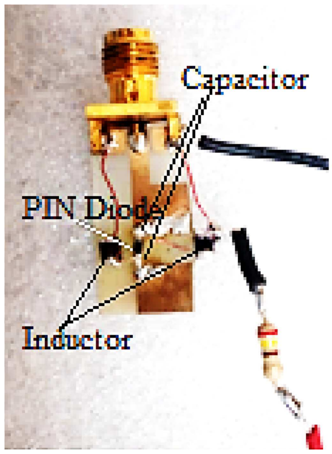

Figure 7. Actual demonstration of the proposed patch antenna (with single PIN diode).

4. Simulation and measurement results

The present section discusses the performance characteristics of the antenna, which was analyzed by an HPEEs of (ADS-momentum). The reflection loss (S_{11}) analysis of the high-frequency S-parameters is the most frequently used simulation to analyze the antenna and any other microwave circuital performance. The patch was fabricated as per the proposed dimensions and it is delineated in Figure 7. The fabricated structure (Figure 7) measured 23 mm wide and 26 mm long (with the area of approx. 595 mm^2) including the probe connector via an outer periphery. The highly compact design area was totally superior to other designs.

The results obtained from the simulation were compared with the measured results of the implemented structure, which proved the consistency of the design analysis with the practical scenario. Far-field results were also obtained for a 3-dimensional radiation pattern.

4.1. Tuning and radiation characteristics of the proposed reconfigurable patch antenna

The obtained results indicated that the variation of S-parameter (S_{11} in dB) with frequency had four operating frequency resonances (Figure (8)). When the switch was turned ON and OFF, the antenna operated in a dual operating band and desired return loss was obtained. The operating frequency ranges of the antenna were found to be as follows: 3.1 to 3.6 GHz and 6 to 8.8 GHz in ON state, and 3.8 to 5.05 GHz and 7.55 to 9 GHz in OFF state of diodes. Table 2 summarizes all the three cases of reconfiguration based on modes of the PIN diode switches. Due to the symmetry of the patch design as well as the placement of both PIN switches, the ON condition of any one of the diodes resulted in the same analysis.

The regular distribution of the spectrum including both the ON and OFF conditions of the proposed design completed the spans of the S and C bands including the most sought WLAN, Wi-Max, and Wi-Fi applications. The ON mode of the PIN diodes shortened the wider upper edges of the patch and this expanded the overall length (L) of the antenna (Figure 5), causing it to resonate at a slightly lower frequency. This inherently brought reconfigurability to the tuning characteristic of the proposed antenna design.

4.2. Gain, power, and efficiency analysis using far-field radiation pattern in the XZ plane ($\phi = 0°$, with both diodes OFF : 4.2 GHz operation)

The far-field simulations were performed using momentum and EMDS (Electro-Magnetic Design Simulator) of ADS (from Keysight Technologies). 3-D radiation patterns with theta (θ) and phi (ϕ) variations are shown in Figure 9 for the PIN switches in ON condition. Figure 10 depicts the 2-D polar radiation plots for 4.2 and 5.04 GHz, which validate both the ON and OFF conditions of the PIN switches. The results could also be generalized to other resonating spectra of the proposed design as the feeding and geometrical design for the antenna remained the same. The symmetry of the far-field radiation pattern over the azimuth plane, over theta (θ), is easily observed in the 3-D simulation results in Figure 9. This mainly occurs due to the

Table 2. Antenna operational tuning range for PIN diode modes configurations.

	Simulated (Monmentum@ADS)	Measured
Diodes OFF	**Centered at 4.2 GHz and 8.1 GHz** - Two bands from 3.8 to 5.05 GHz, and 7.55 to 9 GHz	Centered at 4.3 GHz and 8.05 GHz
Diodes ON	**Centered at 3.35 GHz, 5.04 GHz, 5.56 GHz, and 6.5 GHz** - Total 4 bands from 3.1 to 3.6 GHz, 4.9 to 5.2 GHz, 5.33 to 5.7 GHz, and 6 to 8.8 GHz	Centered at 3.05 GHz and 8.05 GHz
D_1 ON, D_2 OFF	5.12 GHz (with and without radome structure)	–

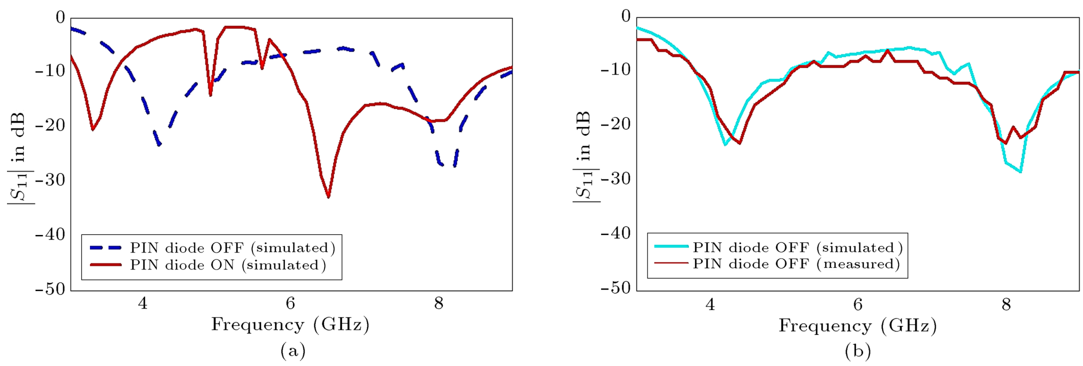

Figure 8. (a) Simulated S_{11} (dB) with PIN diodes ON (solid line) and OFF (dotted line). (b) Comparison of the simulated S_{11} (dB) with the measured result in PIN diodes OFF condition.

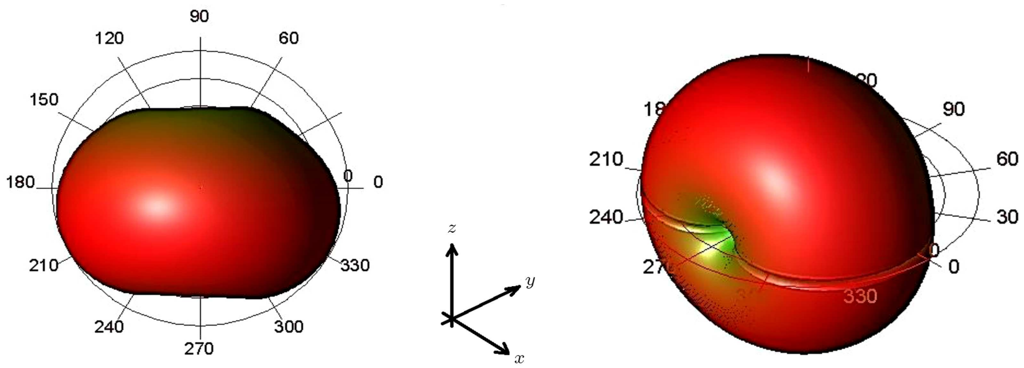

Figure 9. Far-field 3-D radiation pattern of the proposed antenna for 3.35 GHz and 5.56 GHz (diodes/switches ON).

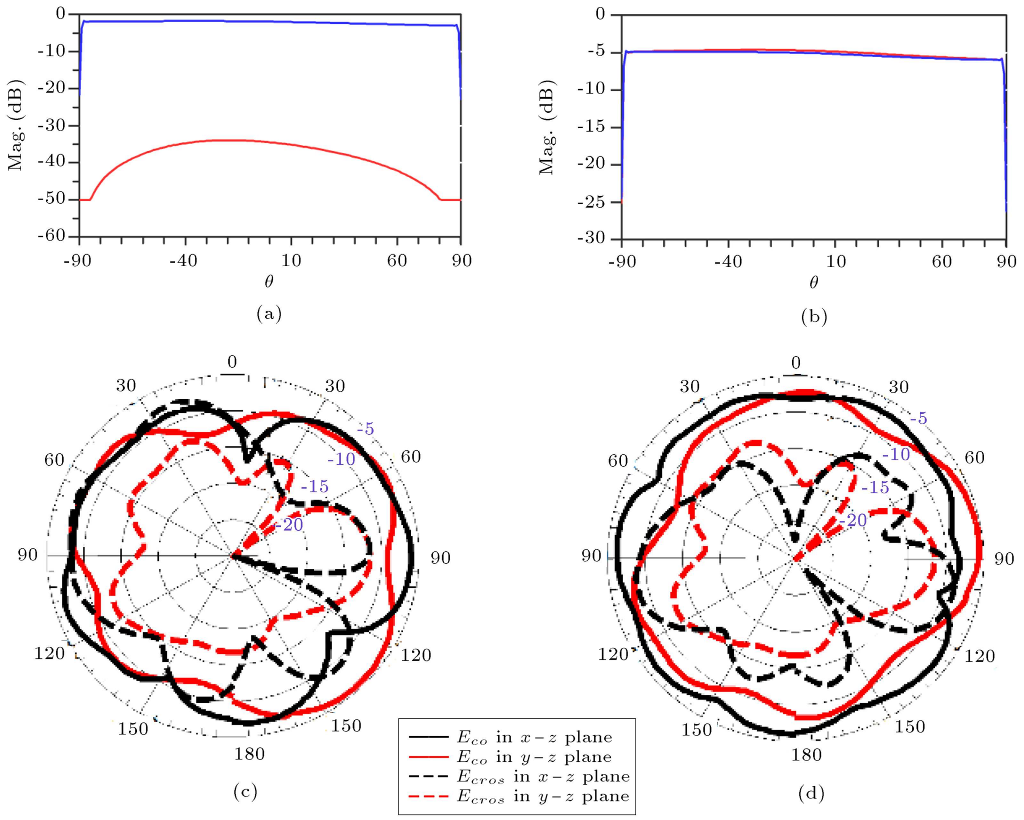

Figure 10. Radiation patterns of the proposed patch antenna: (a) Far-field magnitude of the linear polarization (at 5.04 GHz), (b) far-field magnitude in circular polarization (at 5.04 GHz), (c) 2-D pattern in polar co-ordinates at 4.2 GHz (diodes/switches OFF), and (d) 2-D pattern in polar co-ordinates at 5.04 GHz (diodes/switches ON).

symmetry of the design and symmetry in the feeding mechanism as well (the inset feed discussed in the previous section).

Various fields components are shown in Figure 10 for both linear and circular polarization patterns in far-field. The dominance of the cross-sectional component in the linear polarization enables the design to offer a higher gain in the radial direction [34,35]. The inset feed mechanism also brings in a higher gain in terms of both power and directivity.

Figure 10(c) and (d) also shows the simulated 2-D radiation patterns for the proposed patch antenna with inset feed at the resonant frequency of 4.2 GHz and 5.04 GHz in the $x-z$ ($\phi = 0°$) and $y-z$ ($\phi = 90°$) planes. It completely covers the ON and OFF conditions of the PIN diodes. The simulated co-polarization and cross-polarization radiation patterns for the patch antenna are demarcated with different color lines. It is observed that the measured antenna gain varies from -1.9 to 2.3 dBi with peak efficiency of 89%. The maximum gain is 2.3 dBi with efficiency of 89% at 5.04 GHz and the lowest gain is -1.9 dBi with efficiency of 48% at the frequency of 4.2 GHz. To further support the radiation pattern performance of the proposed antenna

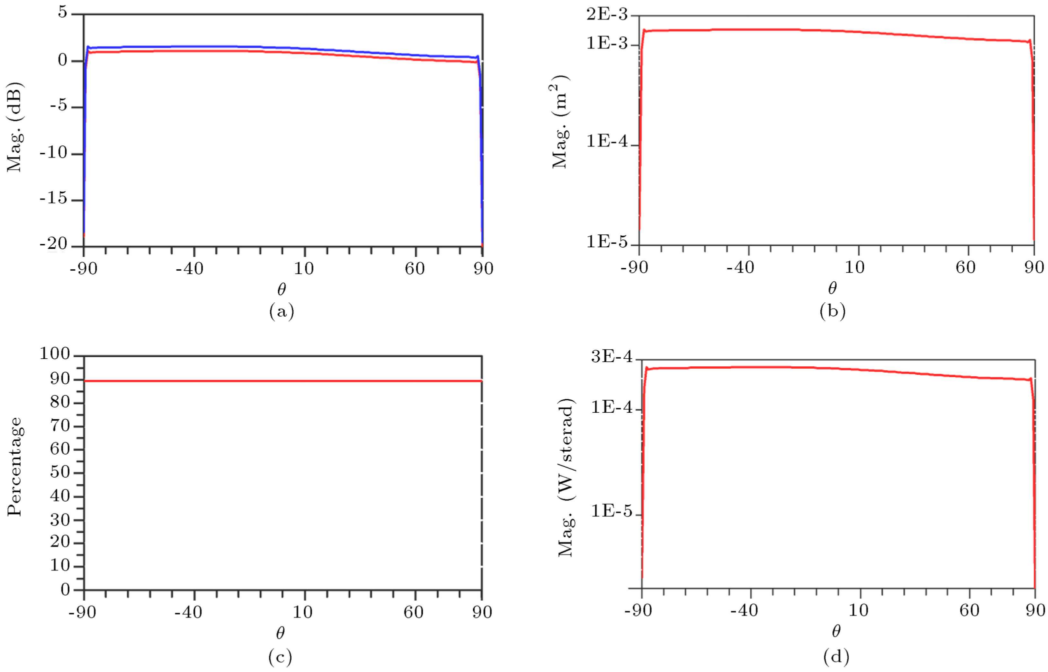

Figure 11. Simulated antenna parameters in the far-field pattern at 5.04 GHz: (a) Power gain (red), (b) directivity (blue) effective areas, (c) antenna efficiency in percentage, and (d) radiated power.

design, the power gain, directivity, and efficiency of the antenna were also analyzed and plotted at 5.05 GHz by a Momentum/EMDS (ADS), as shown in Figure 11.

Some important parameters of the antenna (especially in the far-field pattern) are simulated and analyzed in Figure 11, which demonstrates a higher gain of 2.3 dBi along the azimuthal plane at the frequency of 5.04 GHz, which gives the best efficiency (Figure 11 (a)). The obtained efficiency for theta direction was 89%, which proved the novelty of the design once more with its compact structure. Uniformity of the radiation pattern along the azimuth plane with theta (θ) variation made possible the applicability of the design to multi-band and large-coverage modes, especially in a fading environment [36–38], which is a major concern in the modern RF scenarios [39,40].

4.3. *Effect of radome structure and its thickness variation (D_1 ON and D_2 OFF at 5.12 GHz operation)*

To study the effect of radome structure on antenna gain and radiation pattern, the EMDS simulation environment was conducted under the ADS platform. The same proposed patch antenna in this section was stimulated this time the designed radome structure included. The obtained reflection coefficient (S_{11}) is given in Figure 12 along with the smith chart visualization of the complex behavior of the reflection coefficient (Figure 12(b)). The complete structure was subject to EMDS simulation to analyze the effect of the radome. The radome structure was placed over the microstrip antenna and its impact on the tuning characterization was obtained by a sample simulation set of D_1 ON and D_2 OFF conditions.

The presence of the ABS based radome structure brought in reduction in gain by 4 dB, whereas the radiation pattern and tuning range remained unaffected (Figure 12). This was due to the proper selection of the radome structure material, dimensions, and orientation. A small upper shift in the very-high-frequency tuning of the patch antenna (around 6 to 9 GHz) was observed, but with an insignificant change in the impedance bandwidth. The proposed patch design was compared with several other contemporary design work in recent years for similar spectrum applications. The comparison is presented in Table 3, which highlights the distinguished features and achievements of the antenna including multi-band reconfigurable operation, wide-band coverage, low-cost implementation, effective inset-feeding, and compact die size.

5. Conclusion

A broadband on-chip frequency-reconfigurable antenna with PIN diode switches was presented for S and C-band applications and the effect of ABS-based radome structure on radiation pattern and power efficiency was also studied. The frequency reconfigurability feature of the switching characteristic in the PIN diodes was investigated. With these switches, the proposed antenna obtained an attractive -10 dBi impedance bandwidth of 1450 MHz at 8.1 GHz and 2800 MHz at 6.5 GHz, out of 6 bands of operation. The superior performance at the 2800 MHz bandwidth corresponded

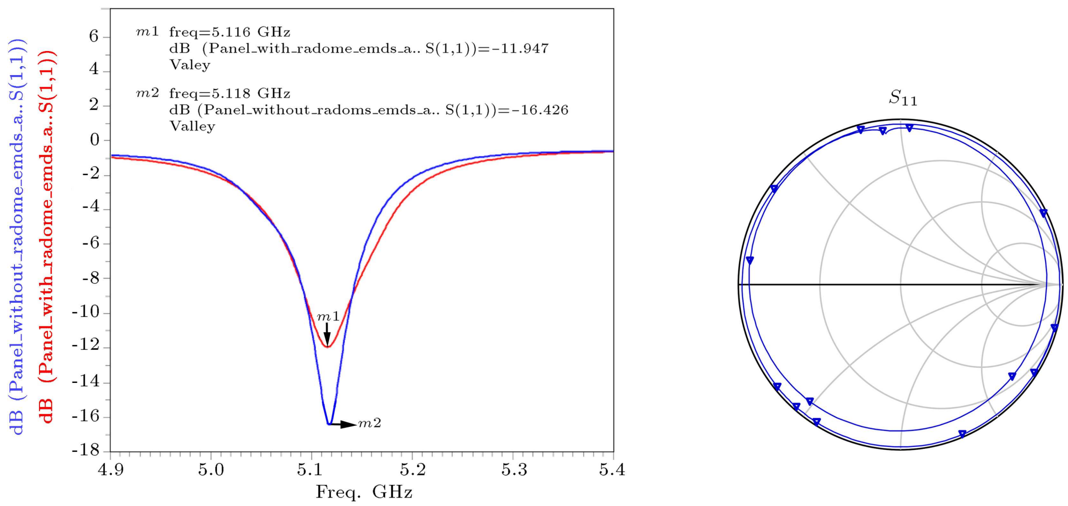

(a) (b)

Figure 12. (a) Simulated S_{11} (dB) in PIN diode 1 ON and diode 2 OFF conditions without radome (blue) and with radome structure (red). (b) Smith chart demonstration for complex reflection S_{11} for 4.9 GHz to 5.7 GHz.

Table 3. Performance comparison of the proposed design with other contemporary and recent designs.

References	[34]	[35]	[36]	[37]	[38]	[39]	[40]	[41]	[42]	[43]	This work*
Area (mm^2)	3900	675	1852.3	400	1720	1892	337.5	2400	7200	1370	595
Substrate	FR4	RO4350B	RO4350	FR4	FR4	PET	FR4	FR4	FR4	RO5880	RO5880
Thickness (mm)	1.55	0.8	1.5	0.8	1.6	0.1	0.8	1.6	1.6	1.57	0.787
No. of resonances	6	6	4	3	3	3	2	12	2	1	6
No. of switches	6	3	5	3	4	1	N/A	4	N/A	N/A	2
BW at different resonance bands (MHz)	1400 to 4600	100; 120; 280; 220; 100; 320	690; 300; 740; 620	210; 400; 580	500; 380; 800	160; 180; 270	1575; 244	1200; 900; 600; 500; 700; 260; 400; 400; 500; 800; 800; 700	1300-2600 (dual band)	1980-4000 (centre: 3 GHz)	1200; 1450; 500; 300; 270; 2800
Tuning efficiency (best case)	57.5%	33.5%	39%	37.8%	38%	30.6%	41.5%	28.8%	66%	66%	43.1% (2800 MHz at 6.5 GHz)
Application	WiFi and Wimax	2G and 3G band	WLAN, Wimax	3G, 4G spectrum	WLAN, Wimax, C-band & ITU	3G, 4G spectrum	Smartphone applications	WLAN, Wimax, X-band satellite	Multi-band MIMO applications	Monopulse radar	S and C band (WLAN)
Special features	Frequency tunable, cedar-shaped	Slot antenna, compact design	Pattern recon-figurable antenna	Miniaturized microstrip antenna	Switchable stubbed ground structure, monopole, triple-band	Narrowband microstrip slot antenna	Use of common metal rim	Cedar-shaped, ultra wideband, CPW fed	Recon-figurable MIMO antenna, 4-slots, 12-dB isolation	Reconfigurable radiation patterns, Inverted U-slots, peak gain of 9.6 dBi	Inset feed, wideband and compact design with radome structure

to 43.08% tuning at the central frequency of 6.5 GHz. This remarkable achievement was a result of the dual-edge shaped patch antenna and centered inset feed implemented in this work. A reasonably high gain (peak gain value) of 2.3 dBi at 5.04 GHz was obtained in the simulation and measurement results. This proved the validity of the proposed on-chip patch design and its simulated behavior along with the inset feed mechanism. Particularly, the modeling of the on-chip switches was generally reliable. The proposed antenna was studied and optimized in different reconfigurable scenarios and especially the effect of radome structure was investigated. The designed patch antenna was studied in terms of important parameters, including reflection, antenna gain, and radiation pattern through simulation as well as measurements. This antenna with a highly compact size of 595 mm^2, radiates efficiently at all the desired bands. Design simplicity,

compactness, and reconfigurability are the features that make this antenna a good choice for future wireless communication applications.

References

1. Shakhirul, M.S., Jusoh, M., Lee, Y.S., et al. "A review of reconfigurable frequency switching technique on microstrip antenna", *J. Phys. Conf. Ser.*, pp. 1019–012042 (2018).
2. Rahman, M., Naghshavarian, M., Mirjavadi, S.S., et al. "Compact UWB band-notched antenna with integrated bluetooth for personal wireless communication and UWB applications", *Electronics*, **8**(2) 158 (2019).
3. Li, T., Zhai, H., Li, L., et al. "Frequency-reconfigurable bow-tie antenna with a wide tuning range", *IEEE Antennas Wireless Propagation Letter*, **13**, pp. 1549–1552 (2014).
4. Korosec, T., Ritosa, P., and Vidmar, M. "Varactor-tuned microstrip-patch antenna with frequency and polarization agility", *Electronics Letter*, **42**, pp. 1015–1017 (2006).
5. Korosec, T., Naglic, L., Tratnik, J., et al. "Evolution of varactor-loaded frequency and polarization reconfigurable microstrip patches", In *Proceedings of the IEEE Asia-Pacific Microwave Conference, Melbourne, VIC, Australia*, **5–8**, December, pp. 705–708 (2011).
6. Singh, R., Slovin, G., Xu, M., et al. "A reconfigurable dual-frequency narrowband CMOS LNA using phase-change RF switches", *IEEE Transaction Microwave Theory and Techniques*, **65**, pp. 4689–4702 (2017).
7. Nguyen-Trong, N., Piotrowski, A., Hall, L., et al. "A frequency- and polarization-reconfigurable circular cavity antenna", *IEEE Antennas Wireless Propagation Letter*, **16**, pp. 999–1002 (2017).
8. Cheema, H.M. and Shamim, A. "The last barrier: On-chip antennas", *IEEE Microwave Magazine*, **14**(1), pp. 79–91 (2013).
9. Karim, M.F. "Integration of SiP-based 60-GHz 4 × 4 antenna array with CMOS OOK transmitter and LNA", *IEEE Transaction Microwave Theory and Techniques*, **59**(7), pp. 1869–1878 (2011).
10. He, F.F., Wu, K., Hong, W., et al. "Low-cost 60-GHz smart antenna receiver subsystem based on substrate integrated waveguide technology", *IEEE Transaction Microwave Theory and Techniques*, **60**(4), pp. 1156–1165 (2012).
11. Liu, C.C. and Rojas R.G. "V-band integrated on-chip antenna implemented with a partially reflective surface in standard 0.13-μm BiCMOS technology", *IEEE Trans. Antennas Propagation*, **64**(12), pp. 5102–5109 (2016).
12. Pilard R. and Montusclat S. "Folded-slot integrated antenna array for millimeter-wave CMOS applications on standard HR SOI substrate", In *Proc. IEEE SiRF*, pp. 1–4 (2009).
13. Nezhad Ahmadi, M.R., Fakharzadeh, M., Biglarbegian B., et al. "High-efficiency on-chip dielectric resonator antenna for mm-wave transceivers", *IEEE Trans. Antennas Propagation*, **58**(10), pp. 3388–3392 (2010).
14. Gao, P., Wang, N., and Chen, Z.N. "A Q-band very broadband on-chip antenna for Q-LINKPAN applications", In *15th International Conference. Electronic Packaging Technology (ICEPT)*, pp. 1344–1346 (2014).
15. Samarthay, V., Pundir, S., and Lal, B. "Designing and optimization of inset fed Rectangular Microstrip Patch Antenna (RMPA) for varying inset gap and inset length", *International Journal of Electronics and Electrical Engineering*, ISSN 0974-2174 **7**(9), pp. 1007–1013 (2014).
16. Balodi, D., Verma A., and Govindacharyulu, P.A. "A high gain low noise amplifier design & comparative analysis with other MOS-topologies for bluetooth applications at 130 nm CMOS", *IEEE Industrial Electronics and Applications Conference (IEAcon)*, **248**, Paper ID: 1570300438, Malaysia (2016).
17. Hedayati, M.K., Abdipour, A., Shirazi, R.S., et al. "Challenges in on-chip antenna design and integration with RF receiver front-end circuitry in nanoscale CMOS for 5G communication systems", *IEEE Access*, 2905861, **7**, March (2019).
18. Pandhare,R. and Abegaonkar, M. "Inset-feed frequency reconfigurable compact e-shape patch with DGS", *Progress in Electromagnetics Research*, **101**, pp. 119–132 (2020).
19. Boukarkar, A., Lin, X.Q., Jiang, Y., et al. "A compact frequency-reconfigurable 36-states patch antenna for wireless application", *IEEE Antennas and Wireless Propagation Letters*, **17**(7), pp. 1349–1353 AWPL-05-18-0891.R1 (2018).
20. Song, Y., Xu, Q., Tian, Y., et al. "An on-chip frequency reconfigurable antennafor Q-band broadband applications", *IEEE Antennas and Wireless Propagation Letters*, **16**, pp. 2232–2235 (2017). DOI: 10.1109/LAWP.2017.2709911
21. Singh, J. "Inset feed microstrip patch antenna", *IJCSMC*, **5**(2), pp. 324–329 (2016).
22. Diogenes, Marcondes, F., Wilson, A., Artuzi, Jr., et al. "A PIN diode model for finite element time domain simulations", *Fundação Araucária with a PIBIC research* (2007).
23. Smith, D., Pendry, J., and Wiltshire, M. "Metamaterials and negative refractive index", *Science*, **305**(5685), pp. 788–792 (2004).
24. Nazir, M.U., Kashif, M., Ahsan, N., et al. "PIN diode modelling for simulation and development of high-power limiter, digitally controlled phase shifter and high isolation SPDT switch", *Proceedings of 2013 10th International Bhurban Conference on Applied Sciences & Technology (IBCAST)*, January, pp. 439–445 (2013).
25. Application Note "Design with PIN Diodes", *M/A-COM Technology Solutions Inc (MACOM), AG312* (1997).
26. Lindell, I.V., Tretyakov, S., Nikoskinen, K., et al. "BW media with negative parameters, capable of supporting

backward waves", *Microwave and Optical Technology Letters*, **31**(2), pp. 129–133 (2001).

27. Ziolkowski, R.W. and Heyman, E. "Wave propagation in media having negative permittivity and permeability", *Physical Review*, **64**(5), p. 056625 (2001).

28. Weng, Z.B., Wang, N.B., and Jiao, Y.C. "Study on high gain patch antenna with metamaterial cover", In *Antennas, Propagation & EM Theory*, ISAPE'06. 7th International Symposium on. IEEE, pp. 1–2 (2006).

29. Hu, J., Yan, C.S., and Lin, Q.C. "A new patch antenna with metamaterial cover", *Journal of Zhejiang University SCIENCE A*, **7**(1), pp. 89–94 (2006).

30. Walton, J., *Radome Engineering Handbook: Design and Principles* , Marcel Dekker Inc, New York City (1970).

31. Luo, G.Q., Hong, W., Tang, H.J., et al. "Filtenna consisting of horn antenna and substrate integrated waveguide cavity FSS", *IEEE Trans. Antennas Propag.*, **55**(1), pp. 92–98 (2007).

32. Koleck, T., Diez, H., and Bolomey, J.C. "Techniques for analyzing finite frequency selective surfaces", In *10th International Conference on Antennas and Propagation*, Conference Publication, **436**, IEE (1997).

33. Hirsch, H. and Grove, D.C. "Practical aimulation of radar antennas and radomes", *Artech House*, Norwood (1988).

34. Madi, M., Al-Husseini, M., Kabalan, K.Y. "Frequency tunable cedar-shaped antenna for WiFi and Wimax", *Prog. Electromagnetics. Res. Lett.*, **72**, pp. 135–143 (2018).

35. Han, L., Wang, C., Chen, X., et al. "Compact frequency reconfigurable slot antenna for wireless applications", *IEEE Antennas Wireless Propagation Letter*, **15**, pp. 1795–1798 (2018).

36. Li, P.K., Shao, Z.H., Wang, Q., et al. "Frequency and pattern reconfigurable antenna for multi-standard wireless applications", *IEEE Antennas Wireless Propagation Letter*, **14**, pp. 333–336 (2015).

37. Borhani M., Rezaei P., and Valizade A. "Design of a reconfigurable miniaturized microstrip antenna for switchable multiband systems", *IEEE Antennas Wireless Propagation Letter*, **15**, pp. 822–825 (2016).

38. Liu, X., Yang, X., and Kong, F. "A frequency-reconfigurable monopole antenna with switchable stubbed ground structure", *Radio Eng. J.*, **24**, pp. 449–454 (2015).

39. Majid, H.A., Rahim, M.K.A., Hamid M.R. et al. "A compact frequency-reconfigurable narrowband microstrip slot antenna", *IEEE Antennas Wireless Propagation Letter*, **11**, pp. 616–619 (2012).

40. Xu, Z., Ding, C., Zhou, Q., et al. "A dual-band dual-antenna system with common-metal rim for smartphone applications", *Electronics*, **8**, p. 348 (2019).

41. Khan, T., Rahman, M., Akram, A., et al. "A low-cost CPW-Fed multiband frequency reconfigurable antenna for wireless applications", *Electronics*, **8**, p. 900 (2019).

42. Zhao, X. and Riaz, S. "A dual-band frequency reconfigurable MIMO patch-slot antenna based on reconfigurable microstrip feedline", *IEEE Access*, **6**, pp. 41450–4145, ACCESS.2018.28584427 (2018).

43. Radavaram, S. and Pour, M. "Wideband Radiation Reconfigurable Microstrip Patch Antenna Loaded with Two Inverted U-Slots", *IEEE Transactions on Antennas and Propagation*, **67**, (3), pp. 1501–1508, March (2019).

Biographies

Rahul Kumar Verma is an Assistant Professor in the Department of ECE at Amity University Uttar Pradesh, Noida UP. He is pursuing PhD in Electronics Engineering at AKTU (formerly UPTU), Lucknow. Mr. Rahul has been serving in the academic area (Amity University, UP) for the past 11 years in the area of antenna and microwave devices.

Ram L. Yadava is Professor in the Department of ECE, Galgotias College of Engineering and Technology, Gr. Noida, U.P. during his doctoral work, he was as associated with and R & D project funded by DST, Government of India. After receiving the PhD degree, he joined VIT University, Vellore T.N, in 2001 and served as the head of the Microwave Division, R & D coordinator and coordinator (UG) of Electrical Sciences. During his service at VIT, he was deputed as a visiting faculty member to Kigali University, Kigali Center Africa. He has also been coordinator of the MTech programme of the U.P. Technical University, 2007-2008. Dr. Yadava has organized several guest lectures, short-term training programmes, FDPs, and conferences in the field of microwaves and antennae. His research areas includes waveguides, microwaves, and microstrip antennae. He has guided several MTech dissertations and five PhDs. He has 120 publications in international/national journals, conferences, and symposiums. He is a member of ISTE, SEMCE (I), and IEEE.

Deepak Balodi, currently working as an Associate Professor in Electronics Engineering in BBD Educational Group-Lucknow, has been practicing and researching in the field of Analog and RF Integrated Circuits for more than 12 years. Mr. Balodi completed his PhD in the year 2020 in the RF-CMOS field and prior to this, he obtained his MSc degree in Integrated Circuits from Central University, Hyderabad. He has authored two books in electrical and electronic circuits and published several papers in reputed journals. Mr. Balodi has been working with various national and international academic bodies like the Central University-Hyderabad, Semi-Conductor Laboratory-Mohali, IET-UK, and Amity University-Noida in his 15 years of academic and teaching career.